Electronic Supplementary Information (ESI)

Robust metal-organic framework with rich electronegative sites for removal of CO_2 from a ternary $C_2H_2/C_2H_4/CO_2$ mixture

Cheng Xiong[1†], Yan-Hong Xiao[1†], Qingyou Liu[2], Ling Chen[1], Chun-Ting He[1], Qing-Yan Liu[1*] & Yu-Ling Wang[1*]

[1]College of Chemistry and Chemical Engineering, Key Laboratory of Functional Small Molecules for Ministry of Education, Jiangxi Normal University, Nanchang 330022, China. [2]Institute of Geochemistry, Chinese Academy of Sciences, Guiyang 550081, China. [†] These authors contributed equally.

Corresponding Authors (email: ylwang@jxnu.edu.cn; qyliuchem@jxnu.edu.cn)

1. Characterization.

Physical Measurements. FT-IR spectra were recorded from KBr disc on a Perkin-Elmer Spectrum One FT-IR spectrometer ranging from 400 to 4000 cm^{-1}. Thermogravimetric analyses were performed under a nitrogen atmosphere with a heating rate of 10 °C/min using a PE Diamond thermogravimetric analyser. Powder X-ray diffraction analyses were performed on a Rigaku Ultima IV diffractometer with Cu-Kα radiation (λ = 1.5418 Å). Energy Dispersive X-Ray Spectroscopy was performed on a HITACHI S-3400N.

Crystallographic Study. X-ray single-crystal diffraction experiment was carried out a Rigaku Oxford SuperNova diffractometer equipped with an EOS detector (Mo-K*a* radiation, λ = 0.71073 Å). Absorption correction and data reduction were handled with a *CrysAlisPro package*.[1] The *SHELXT-2015* [2] and *SHELXL-2018* [3] were applied to structure solution and refinement. The two fluorine atoms of 2,5-difluoroterephthalic ligand were disordered over two positions. Thus the hydrogen atoms of the 2,5-difluoroterephthalic ligand couldn't be added. All other hydrogen atoms were modelled geometrically and refined with a riding model. Non-hydrogen atoms were refined anisotropically. The guest water and DMF molecules are highly disordered and treated by

SQUEEZE of *PLATON*.[4]

Isosteric heat of adsorption. The gas adsorption isotherms measured at 273 and 298 K were first fitted to a virial equation (equation S1) (Figure S7).[5] Then the Q_{st} values for C_2H_2, C_2H_4 and CO_2 were calculated based on the fitting parameters using equation S2 (Figure S7d).

$$\ln P = \ln N + \frac{1}{T}\sum_{i=0}^{m} a_i N^i + \sum_{i=0}^{n} b_i N^i \qquad \text{(equation S1)}$$

$$Q_{st} = -R\sum_{i=0}^{m} a_i N^i \qquad \text{(equation S2)}$$

where P is pressure(mmHg), N is the adsorbed quantity (mmol g^{-1}), T is the temperature(K), a_i and b_i are virial coefficients, R is the universal gas constant (8.314 J K^{-1} mol^{-1}), and m and n determine the number of coefficients required to adequately describe the isotherm.

Ideal adsorbed solution theory (IAST) calculations of adsorption selectivity. The IAST was used to predict mixed gas behavior from experimentally measured single-component isotherms.[6] The experimentally measured loadings for C_2H_2, C_2H_4 and CO_2 in JXNU-14 were fitted with the single-site Langmuir model (equation S3 and Figure S9).

$$q = q_{A,sat}\frac{b_A p}{1 + b_A p} \qquad \text{(equation S3)}$$

Where p (unit: kPa) is the pressure of the bulk gas at equilibrium with the adsorbed phase, q (unit: mmol g^{-1}) is the adsorbed amount per mass of adsorbent, $q_{A,sat}$ (unit: mmol g^{-1}) is the saturation capacity, b_A (unit: 1/kPa) is the affinity coefficient.

The adsorption selectivity for binary mixture (A and B) using the Langmuir fitting parameters is defined by equation S4.

$$S_{ads} = \frac{q_A / q_B}{y_A / y_B} \qquad \text{(equation S4)}$$

(where the q_A and q_B represent the molar loadings (mmol g^{-1}). The y_A and y_B ($y_B = 1 - y_A$) are the mole fractions in a bulk fluid mixture).

Breakthrough separation experiments. The breakthrough curves were measured on a homemade apparatus for the binary C_2H_2/CO_2 (v:v = 1:1) and C_2H_2/CO_2 (v:v = 1:1) and the ternary $C_2H_2/C_2H_4/CO_2$ (v:v:v = 1:1:1) at 298 K and 1 bar. The gas flows were controlled at the inlet by a mass flow meter as 2 mL min^{-1} for the binary mixtures or 3 mL min^{-1} for the ternary mixtures and a gas chromatograph (TCD-Thermal Conductivity Detector) continuously monitored the effluent

gas from the adsorption bed. Prior to every breakthrough experiment, we activated the sample by flushing the adsorption bed with helium gas for 1 hours at 298 K. Subsequently, the column was allowed to equilibrate at the measurement rate before we switched the gas flow

Table S1. Crystal structure refinement data.

	 C_2H_2	 C_2H_4	 CO_2
Molecule size (Å^3)	3.32 × 3.34 × 5.7	3.3 × 4.2 × 4.8	13.18 × 3.33 × 5.36
Boiling point (K)	188.4	169.4	194.7
Dipole moment (e.s.u. cm)	0	0	0
Quadrupole moment ($\times 10^{-26}$ e.s.u. cm^2)	3.00	1.50	4.30
Polarizability ($\times 10^{-25}$ cm^3)	33.3-39.3	42.52	29.11
Kinetic diameter (Å)	3.300	4.163	3.300

Table S2. Crystal structure refinement data.

	JXNU-14
formula	$C_{42}H_{18}N_6O_{13}F_6Fe_3$
fw	1096.17
temp (*K*)	293(2) K
Radiation	Mo-Kα (0.71073 Å)
cryst syst	hexagonal
Space group	$P6_3/mmc$
Z	2
a (Å)	16.7482(3)
b (Å)	16.7482(3)
c (Å)	15.2933(6)
α (deg)	90
β (deg)	90

γ (deg)	120
V (Å^3)	3715.1(2)
D_{calcd} (g·cm^{-3})	0.980
μ (mm^{-1})	0.636
no. of reflns collected	9894
independent reflns	1456
F(000)	1096
R_{int}	0.0316
R_1 (I >2 σ (I)) [a]	0.0895
wR_2 (I >2 σ (I)) [a]	0.2447
CCDC number	2166003

It should be noted that the counter ions of hydroxide ions are not included into the formula.

[a] $R_1 = \Sigma||F_o| - |F_c|| / \Sigma|F_o|$ and $wR_2 = \{\Sigma[w(F_o^2 - F_c^2)^2] / \Sigma[w(F_o^2)^2]\}^{1/2}$

2. Results and discussion

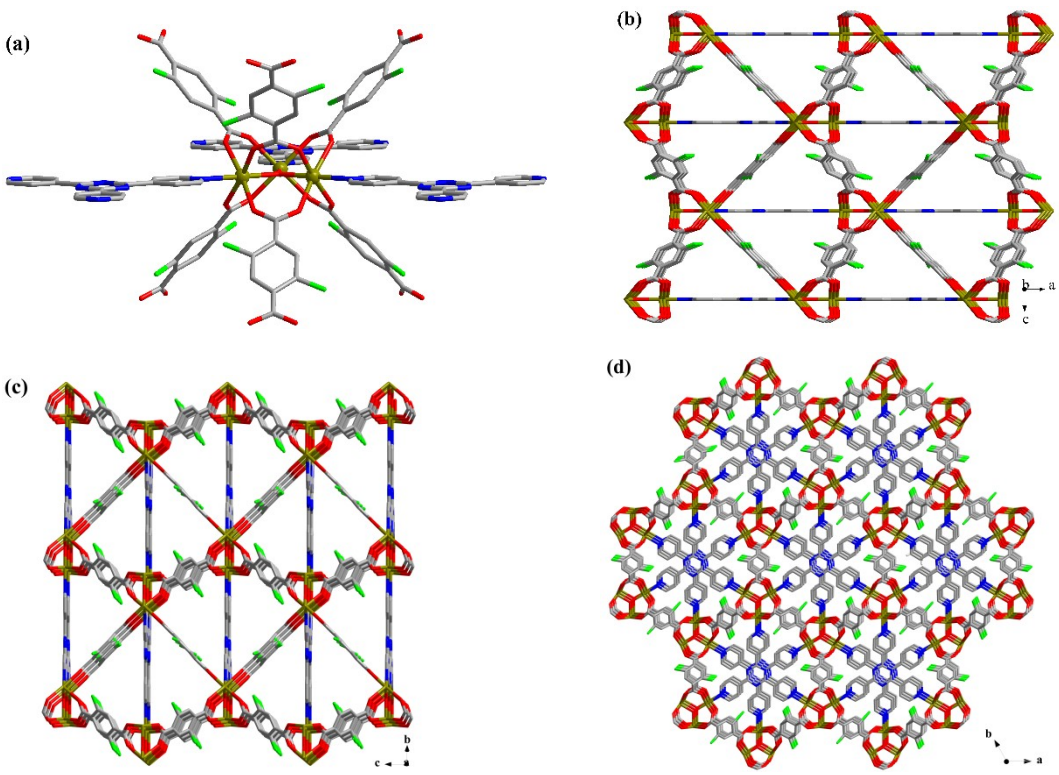

Fig. S1 (a) The trimeric [$Fe_3(\mu_3$-O)] cluster is surrounded by six DFBDC^{2-} and three TPT ligands. (b-d) 3D structure of JXNU-14 showing the 1D channels with triangular aperture (Hydrogen atom are not shown. Fluorine atoms represent as green lines).

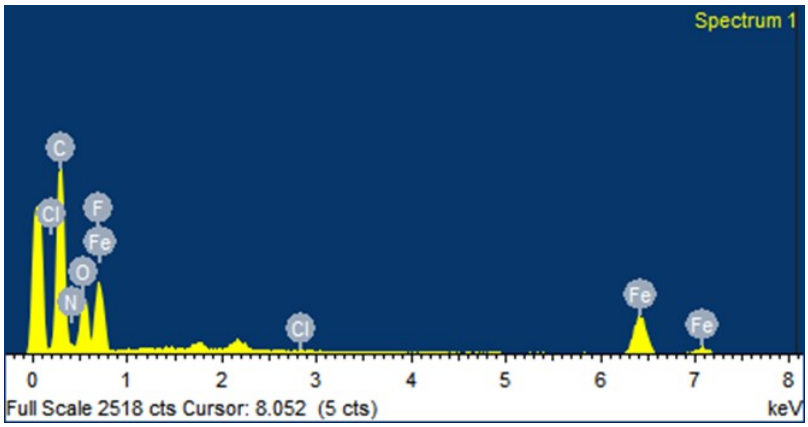

Element	Weight%	Atomic%
C K	45.37	56.26
N K	7.18	7.63
O K	21.54	20.06
F K	17.65	13.84
Cl K	0.03	0.01
Fe K	8.23	2.20
Totals	100.00	

Fig. S2 Energy dispersive X-ray spectroscopy of JXNU-14.

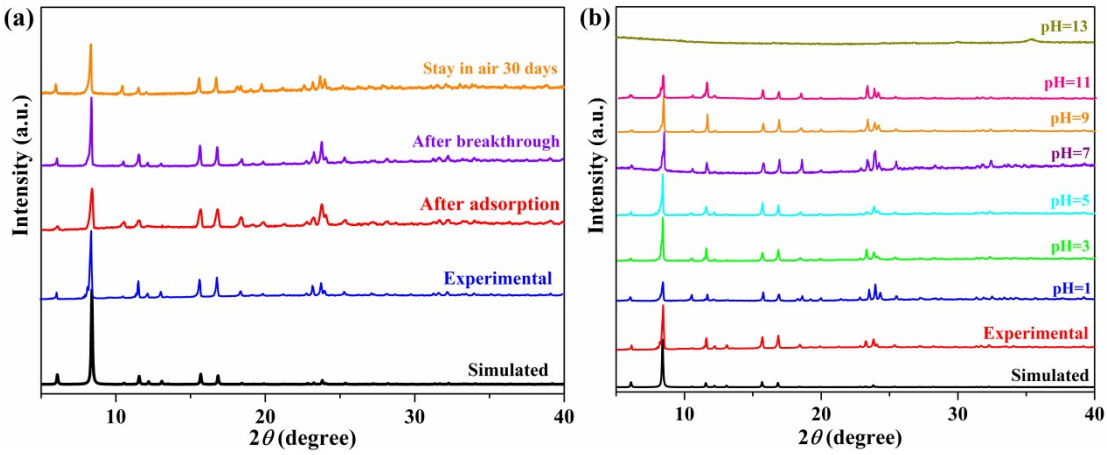

Fig. S3 (a) PXRD patterns of JXNU-14. (b) PXRD patterns of JXNU-14 soaking in aqueous solutions with different pH values.

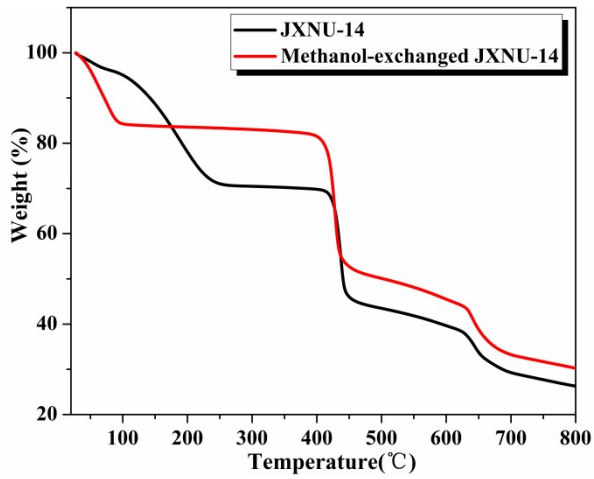

Fig. S4 TGA curves of JXNU-14.

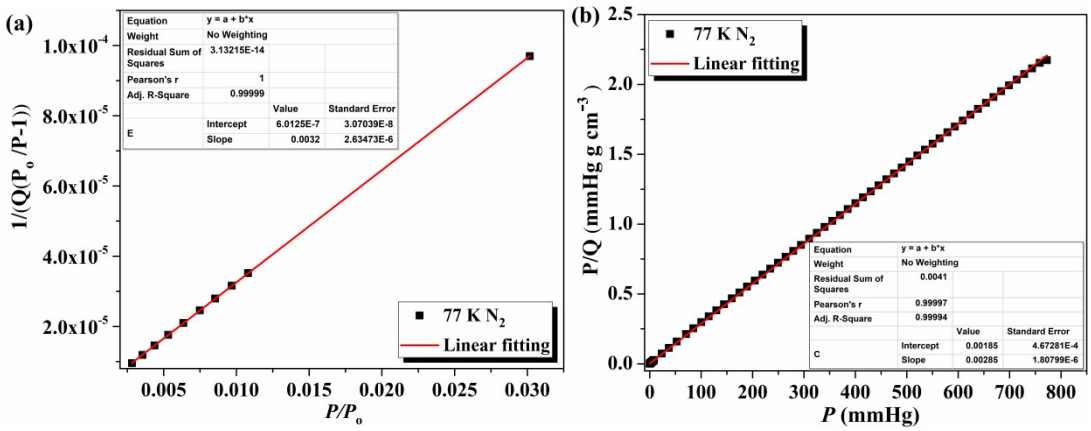

$S_{BET} = (6.023\times10^{23}\times0.162\times10^{-18})/((6.0125\times10^{-7}+0.0032)\times22414) = 1361\ m^2g^{-1}$

$S_{Langmuir} = (6.023\times10^{23}\times0.162\times10^{-18})/(22414\times0.00285) = 1527\ m^2g^{-1}$

Fig. S5 BET surface area plot (a) and Langmuir surface area plot (b) for JXNU-14.

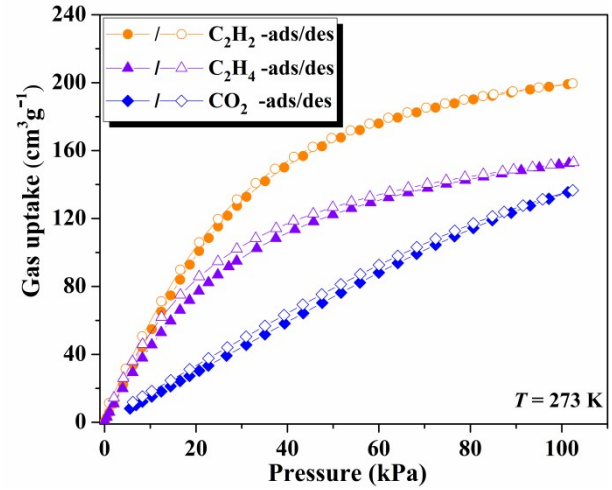

Fig. S6 Adsorption isotherms of JXNU-14 at 273 K.

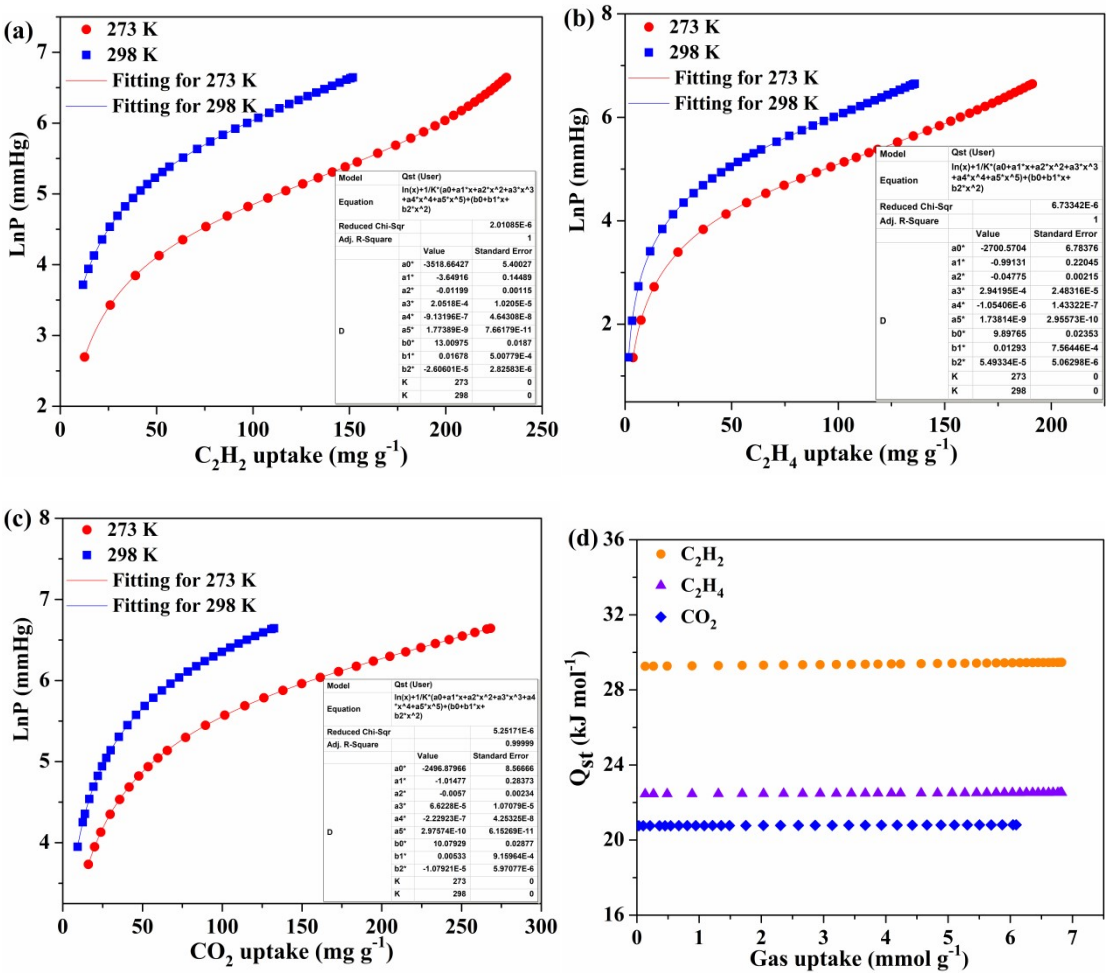

Fig. S7 Virial fits of C_2H_2 (a), C_2H_4 (b) and CO_2 (c) isotherms and (d) Q_{st} for C_2H_2, C_2H_4 and CO_2 in JXNU-14.

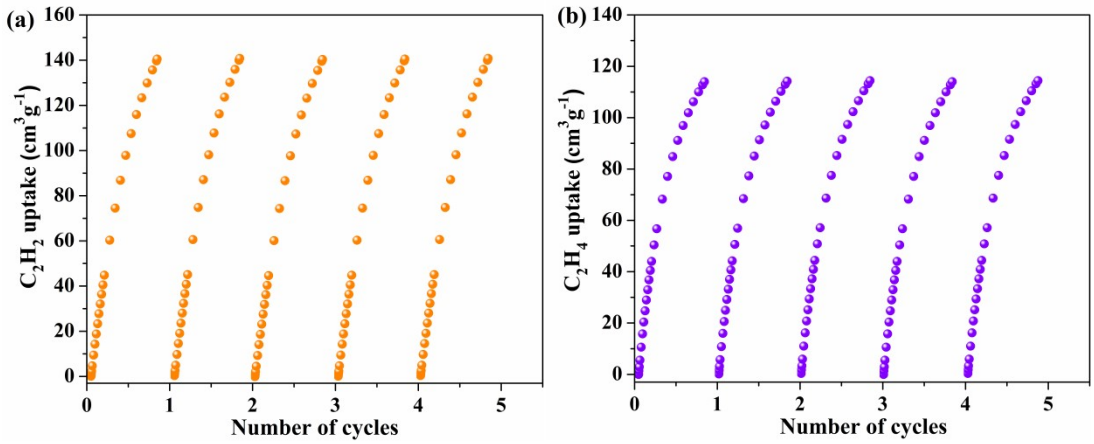

Fig. S8 Cycles of (a) C_2H_2 and (b) C_2H_4 adsorption for JXNU-14 at 298 K.

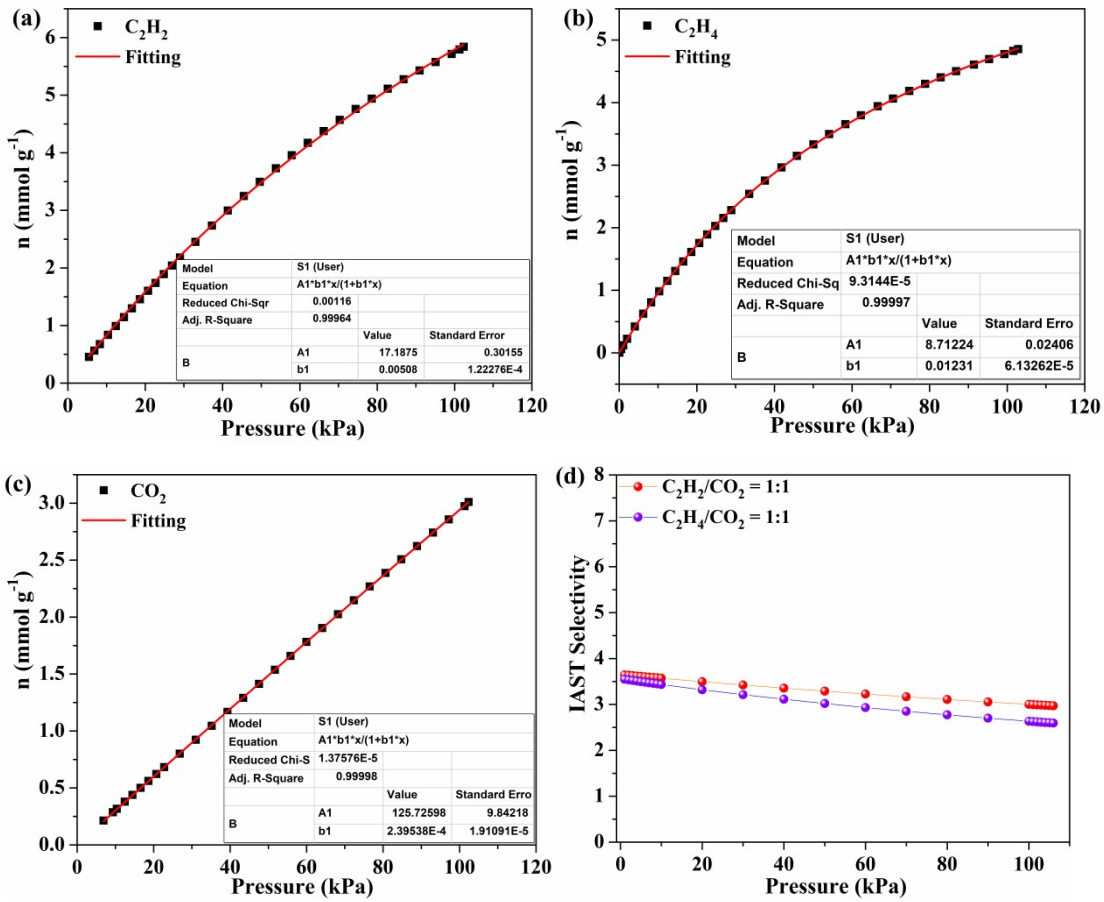

Fig. S9 The graphs of the single-site Langmuir equation fit for adsorption of C_2H_2 (a), C_2H_4 (b) and CO_2 (c) at 298 K on JXNU-14. (d) IAST selectivity for JXNU-14 at 298 K.

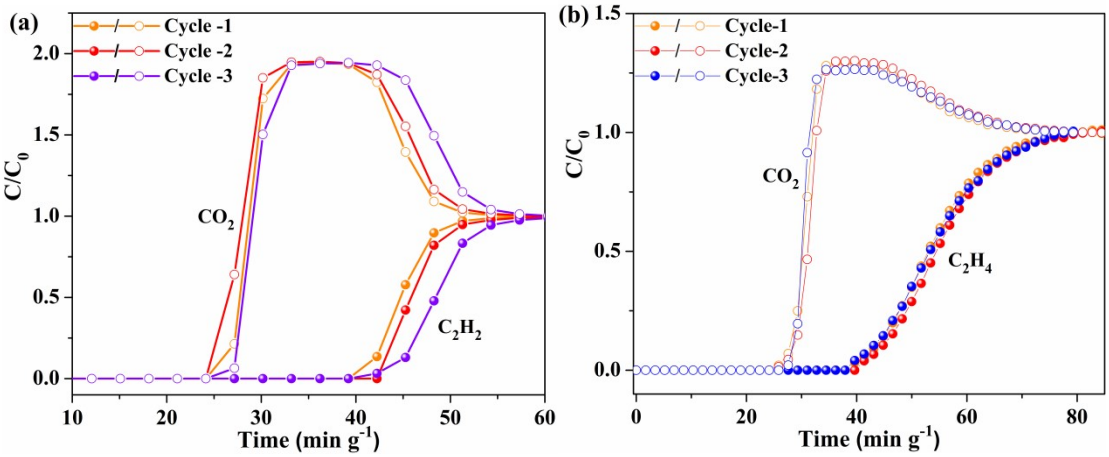

Fig. S10 The cycling breakthrough tests for (a) C_2H_2/CO_2 (1:1) and (b) C_2H_4/CO_2 (1:1) with JXNU-14 (total gas flow: 2 mL min^{-1}).

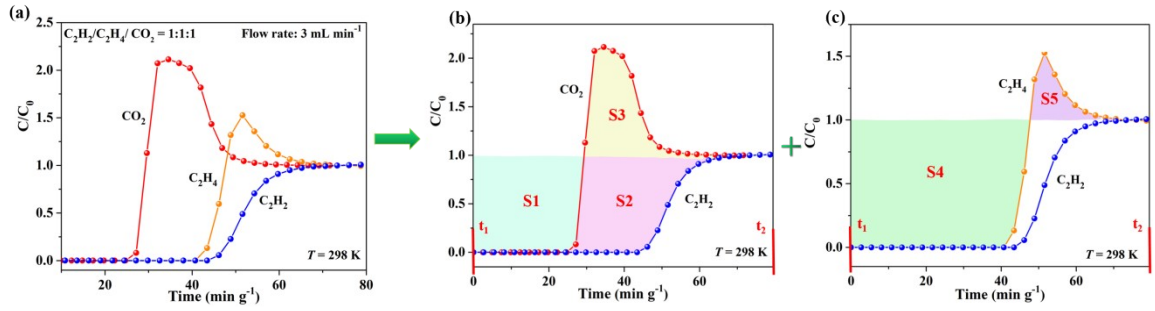

The capture amount (Q_1, mmol g^{-1}) of C_2H_2 during t_0 to t_1 is calculated as:

$$Q_1 = \frac{v \times V\%}{24.5 \times m}\int_{t_0}^{t_1}(c_0 - c_i)dt = \frac{v \times V\%}{24.5 \times m}(S1 + S2)$$

v refers to the total flow rate of the gas mixture, V% refers to the molar fraction of C_2H_2, and m refers to the mass of the adsorbent.

The captured amounts of CO_2 (Q_2, mmol g^{-1}) and C_2H_4 (Q_3, mmol g^{-1}) during t_0 to t_1 can be similarly calculated as

$$Q_2 = \frac{v \times V\%}{22.4 \times m}(S1 - S3) \qquad Q_3 = \frac{v \times V\%}{22.4 \times m}(S4 - S5)$$

Fig. S11 The breakthrough curves of $C_2H_2/C_2H_4/CO_2$ (1:1:1) for JXNU-14 at 298 K.

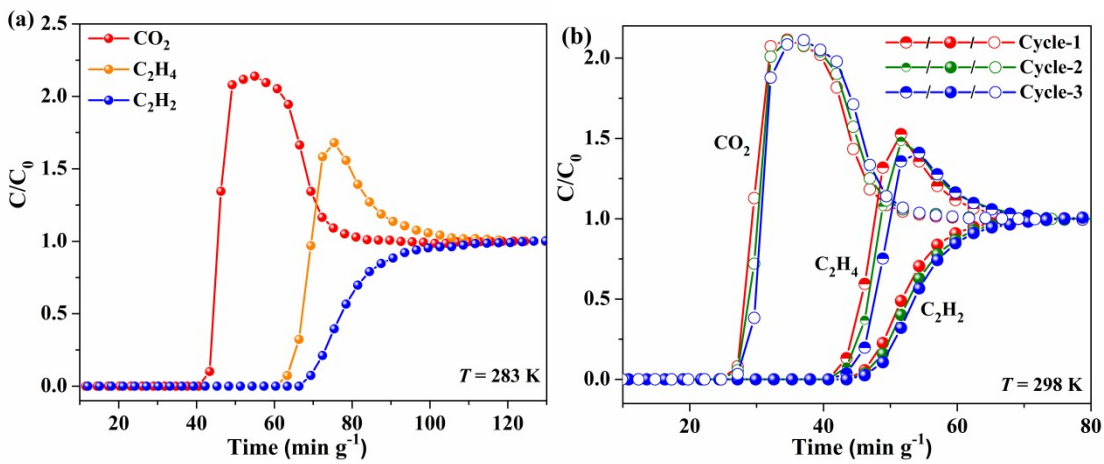

Fig. S12 (a) Breakthrough curves for $C_2H_2/C_2H_4/CO_2$ (1:1:1) mixture with JXNU-14. (b) Cycling breakthrough experiments for JXNU-14 based on $C_2H_2/C_2H_4/CO_2$ (1:1:1) mixture (total gas flow: 3 mL min^{-1})

Table S3. Summary of adsorption uptakes (298 K and 1 bar) and IAST selectivities (C_2H_2/CO_2= 1:1) at 1 bar and 298 K for MOFs mentioned in main text.

Compounds	C_2H_2 uptake (cm^3 g^{-1})	CO_2 uptake (cm^3 g^{-1})	S_{ads}	Ref.
JNU-1	62.1	50.3	3.0	7
SNNU-63	91.1	43.7	2.7	8

FJU-6-TATB	110.0	58.0	3.1	9
UTSA-68a	70.1	39.6	3.4	10
JXNU-14	137.5	67.4	2.97	**This work**

Table S4. Summary of adsorption uptakes (298 K and 1 bar) and IAST selectivities (C_2H_4/CO_2= 1:1) at 1 bar and 298 K for MOFs mentioned in main text.

Compounds	C_2H_4 uptake (cm^3 g^{-1})	CO_2 uptake (cm^3 g^{-1})	S_{ads}	Ref.
SNNU-95	15.3	14.7	2.4	11
ZJNU-120(Sm)	52.7	33.9	2.4	12
MOF-74(Zn)	132.3	124.2	3.3	13
Ni_2(m-dobdc)	145.6	156.8	4.1	14
UTSA-74	103.8	90.5	5.4	15
JXNU-14	110.1	67.4	2.6	**This work**

References

1 CrysAlisPro, Rigaku Oxford Diffraction: The Woodlands, TX. 2015.

2 G. M. Sheldrick *Acta Crystallogr Sect A Found Adv,* 2015, **A71**, 3–8.

3 G. M. Sheldrick. *Acta Crystallogr Sect C Struct Chem*, 2015, **C71**, 3–8.

4 Spek AL. PLATON: A Multipurpose Crystallographic Tool; Utrecht University: Utrecht, The Netherlands. 2001

5 J. L. C. Rowsell and O. M.Yaghi, *J Am Chem Soc*, 2006, **128**, 1304−1315.

6 A-L Myers and J. M.Prausnitz, *AIChE J*, 1965, **11**, 121−127.

7 H. Zeng, M. Xie, Y.-L. Huang, Y. Zhao, X.-J. Xie, J.-P. Bai, M.-Y. Wan, R. Krishna, W. Lu and D. Li, *Angew. Chem., Int. Ed.,* 2019, **58**, 8515−8519.

8 Y.-T. Li, J.-W. Zhang, H.-J. Lv, M.-C. Hu, S.-N. Li, Y.-C. Jiang and Q.-G. Zhai, *Inorg. Chem.,* 2020, **59**, 10368−10373.

9 L. Liu, Z. Yao, Y. Ye, Y. Yang, Q. Lin, Z. Zhang, M. O'Keeffe and S. Xiang, *J. Am. Chem. Soc*. 2020, **142**, 9258−9266.

10 G.-G. Chang, B. Li, H.-L. Wang, T.-L. Hu, Z.-B. Bao and B.-L. Chen, *Chem. Commun*., 2016, **52**, 3494−3496.

11 H.-P. Li, S.-N. Li, X.-Y. Hou, Y.-C. Jiang, M.-C. Hu and Q.-G. Zhai, *Dalton Trans.,* 2018, **47**, 9310−9316.

12 X.-X. Wang, L.-L. Yue, P. Zhou, L.-H. Fan and Y.-B. He, *Inorg. Chem.,* 2021, **60**, 17249−17257.

13 X. Zhang, H. Cui, R.-B. Lin, R. Krishna, Z.-Y. Zhang, T. Liu, B. Liang and B.-L. Chen, *ACS Appl. Mater. Inter.,* 2021, **13**, 22514−22520.

14 J. E. Bachman, D. A. Reed, M. T. Kapelewski, G. Chachra, D. Jonnavittula, G. Radaelli and J.-R. Long, *Energ Environ. Sci.,* 2018, **11**, 2423−2431.

15 X. Zhang, H. Cui, R.-B. Lin, R. Krishna, Z.-Y. Zhang, T. Liu, B. Liang and B.-L. Chen, *ACS Appl. Mater. Inter.,* 2021, **13**, 22514−22520.